Inorganic Chemistry
Article

Inorg. Chem. **2009**, *48*, 9205–9213 **9205**
DOI: 10.1021/ic900886y

Spin-Canting and Metamagnetic Behavior in a New Species from the Hydrothermal Co(II)-*trans*-3-Pyridylacrylate System

Kartik Chandra Mondal,[†] George E. Kostakis,[‡] Yanhua Lan,[†] Christopher E. Anson,[†] and Annie K. Powell*[,†,‡]

[†]*Institut für Anorganische Chemie der Universität Karlsruhe, Karlsruhe Institute of Technology, Engesserstrasse 15, D-76131 Karlsruhe, Germany, and* [‡]*Institut für Nanotechnologie, Forschungszentrum Karlsruhe, Karlsruhe Institute of Technology, Postfach 3640, D-76021 Karlsruhe, Germany*

Received May 7, 2009

Hydrothermal reaction of $CoCl_2$ with *trans*-3-pyridylacrylic acid (3-pycaH) and Et_3N results in the formation of a new three-dimensional network formulated as $[\{Co_4(\mu\text{-}H_2O)_2(3\text{-pyca})_8\}_{0.94}\{Co_5(\mu_3\text{-}OH)_2(3\text{-pyca})_8\}_{0.06}]$. Magnetic measurements reveal that spin-canting and metamagnetic behavior coexist in this compound with a critical temperature at 9.5 K.

Introduction

The first designed synthesis of a multidimensional compound reported by Robson and co-workers two decades ago[1] inspired scientists coming from different backgrounds and opened new avenues to the whole synthetic community. Initially, a wide variety of novel materials was synthesized by utilizing simple metal salts as nodes and bridging organic ligands as linkers. More recently the emphasis has shifted toward using polynuclear clusters instead of single metal ions as nodes, with more complicated polytopic ligands as linkers, in the synthesis of multidimensional compounds. It is well-known that various parameters affect the structure of the final product, although in some cases it is possible to predict the structural propagation by use of designed ligands with specific coordination groups and geometry.[2] There has been a recent increase in interest in such coordination polymers which can be utilized as functional solid materials in catalysis,[3] magnetism,[4] hydrogen storage,[5] and luminescence and chemical sensing.[6]

In the field of molecular magnetism, the magnetic properties of these multidimensional coordination polymers have been correlated with their structures.[7] Polymeric magnetic networks can show three-dimensional (3D) magnetic ordering[8] and sometimes multiple ordering processes, during which the complex undergoes multiple magnetic phase transformations which have their origin in the superexchange in the smallest possible magnetic unit with subsequent propagation through magnetic interactions in the 3D structures.[7,9] When the intermolecular antiferromagnetic interaction is strong enough between magnetic layers, it may align the spins antiferromagnetically, giving an overall spin of zero. However, if the spins are canted rather than collinear, a resultant spin for the particular magnetic unit is seen, and the spins on these units can align ferromagnetically below a certain temperature giving rise to an ordered state.[8−10] This is well-known as canted antiferromagnetism and is also possible for a molecular complex.[11] Single ion magnetic anisotropy as well as Dzyaloshinsky−Moriya antisymmetric superexchange between the anisotropic ions can enhance the spin-canting.[12,13]

*To whom correspondence should be addressed. E-mail: powell@aoc.uni-karlsruhe.de.

(1) (a) Hoskins, B. F.; Robson, R. *J. Am. Chem. Soc.* **1989**, *111*, 5962. (b) Hoskins, B. F.; Robson, R. *J. Am. Chem. Soc.* **1990**, *112*, 1546.
(2) Lehn, J.-M. *Rep. Prog. Phys.* **2004**, *67*, 249.
(3) See for example: (a) Proch, S.; Herrmannsdörfer, J.; Kempe, R.; Kern, C.; Jess, A.; Seyfarth, L.; Senker, J. *Chem.—Eur. J.* **2008**, *14*, 8204. (b) Sun, C.-Y.; Liu, S.-X.; Liang, D.-D.; Shao, K.-Z.; Ren, Y.-H.; Su, Z.-M. *J. Am. Chem. Soc.* **2009**, *131*, 1883.
(4) See for example: (a) Mukherjee, S.; Lan, Y.; Kostakis, G. E.; Clérac, R.; Anson, C. E.; Powell, A. K. *Cryst. Growth Des.* **2009**, *9*, 577. (b) Ouellette, W.; Prosvirin, A. V.; Whitenack, K.; Dunbar, K. R.; Zubieta, J. *Angew. Chem., Int. Ed.* **2009**, *48*, 2140.
(5) (a) Dincă, M.; Long, J. R. *Angew. Chem., Int. Ed.* **2008**, *47*, 6766. (b) Nouar, F.; Eckert, J.; Eubank, J. F.; Forster, P.; Eddaoudi, M. *J. Am. Chem. Soc.* **2009**, *131*, 2864.
(6) See for example: (a) Ye, J.-W.; Wang, J.; Zhang, J.-Y.; Zhang, P.; Wang, Y. *CrystEngComm* **2007**, *9*, 515. (b) Genuis, E. D.; Kelly, J. A.; Patel, M.; McDonald, R.; Ferguson, M. J.; Greidanus-Strom, G. *Inorg. Chem.* **2008**, *47*, 6184.
(7) Yin, P.; Gao, S.; Zheng, L.-M.; Wang, Z.; Xin, X.-Q. *Chem. Commun.* **2003**, 1076.
(8) Cheng, X.-N.; Zhang, W.-X.; Chen, X.-M. *J. Am. Chem. Soc.* **2007**, *129*, 15738.
(9) Humphrey, S. M.; Wood, P. T. *J. Am. Chem. Soc.* **2004**, *126*, 13236.
(10) Bellitto, C.; Federici, F.; Colapietro, M.; Portalone, G.; Caschera, D. *Inorg. Chem.* **2002**, *41*, 709.
(11) Gutschke, S. O. H.; Price, D. J.; Powell, A. K.; Wood, P. T. *Angew. Chem., Int. Ed.* **1999**, *38*, 1088.
(12) Jia, H.-P.; Li, W.; Ju, Z.-F.; Zhang, J. *Chem. Commun.* **2008**, 371.
(13) Li, J.-R.; Yu, Q.; Tao, Y.; Bu, X.-H.; Ribas, J.; Batten, S. R. *Chem. Commun.* **2007**, 2290.

Published on Web 08/31/2009

Scheme 1. Known Coordination Modes for the *trans*-3-Pyridylacrylate (3-pyac)[a]

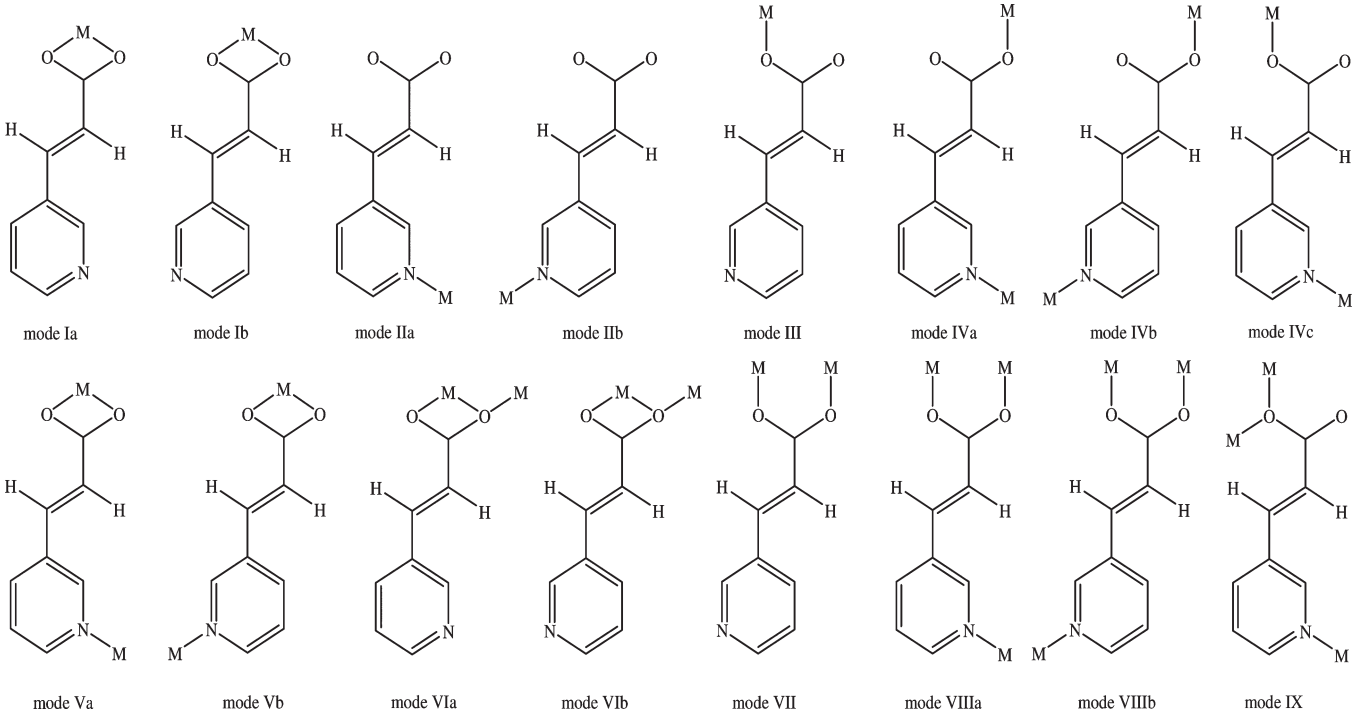

[a] Mode Ia,[18a−c] Mode Ib,[18b,d−g] Mode IIa,[18h−k] Mode IIb,[18i,j,l−p] Mode III,[18c,k,p] Mode IVa,[18h,l] Mode IVb,[18h,i,l] Mode IVc,[18e,i,19a,19b] Mode Va,[18h,i,l,m,19c] Mode Vb,[18l,19d] Mode VIa,[18a,d,e] Mode VIb,[18a,d,e,g,19e] Mode VII,[18f,g,19e] Mode VIIIa,[20a] Mode VIIIb[18e,f,19b,19e,20b,20c] and Mode IX[20a].

Polypyridine[14] and polycarboxylate[15] compounds have been shown to be useful ligands for the synthesis of extended coordination networks. Ligands combining pyridine and carboxylate groups have been previously used for the synthesis of compounds which possess porosity and nonlinear optical activity.[16] One of our major research goals is to construct coordination polymers with an emphasis on their magnetic properties.[4a,17] In this paper we describe the use of *trans*-3-pyridylacrylate (3-pyac) to construct such a compound with Co^{II}. A literature survey reveals that 3-pyac is known to coordinate to one,[18] two,[18a,d−i,l,m,19] or three[18e−g,19b,19e,20] metal centers and because of the rotation of the pyridyl group possesses a large variety of different coordination modes (Scheme 1). Various divalent Mn^{II},[18j,20c] Fe^{II},[18h] Co^{II},[18h−j,o,19b,20c] Ni^{II},[18h,i,19b] Cu^{II},[18e,l,20b] Zn^{II},[18n,19a] Cd^{II},[18n] and Pb^{II}[18n] metal centers have been used with 3-pyac. In particular, for the divalent Co^{II} center, by varying the hydrothermal reaction conditions, 3D $[Co_2(3\text{-pyca})_4(\mu\text{-}H_2O)]\cdot HL\cdot x(H_2O)$ (**1**)[19b] and α-$Co(3\text{-pyca})_2(H_2O)_2$ (**2**),[18h,i] or one-dimensional (1D) β-$Co(3\text{-pyca})_2(H_2O)_2$ (**3**),[18h,i] compounds can be obtained. The structure of **2** possesses two crystallographically unique (but chemically similar) Co^{II} atoms and two unique 3-pyca ligands. The ligands bridge between the metals in a linear fashion with the carboxylate groups coordinating in a monodentate fashion. Each Co lies on a

(14) See for example: (a) Blake, A. J.; Champness, N. R.; Hubberstey, P.; Li, W.-S.; Withersby, M. A.; Schröder, M. *Coord. Chem. Rev.* **1999**, *183*, 117. (b) Kitagawa, S.; Masaoka, S. *Coord. Chem. Rev.* **2003**, *246*, 73.

(15) See for example: (a) Yaghi, O.; O'Keeffe, M.; Ockwig, N. W.; Eddaoudi, M.; Kim, J. *Nature* **2003**, *423*, 705. (b) Tong, M.-L.; Kitagawa, S.; Chang, H.-C.; Ohba, M. *Chem. Commun.* **2004**, 418.

(16) See for example: (a) Evans, O. R.; Lin, W. *Acc. Chem. Res.* **2002**, *35*, 511. (b) Tynan, E.; Jensen, P.; Kruger, P. E.; Lees, A. C.; Nieuwenhuyzen, M. *J. Chem. Soc., Dalton Trans.* **2003**, 1223.

(17) (a) Price, D. J.; Powell, A. K.; Wood, P. T. *J. Chem. Soc., Dalton Trans.* **2000**, 3566. (b) Gutschke, S. O. H.; Price, D. J.; Powell, A. K.; Wood, P. T. *Angew. Chem., Int. Ed.* **2001**, *40*, 1920. (c) Mukherjee, S.; Lan, Y.; Novitchi, G.; Kostakis, G. E.; Anson, C. E.; Powell, A. K. *Polyhedron* **2009**, *28*, 1782. (d) Viertelhaus, M.; Adler, P.; Clérac, R.; Anson, C. E.; Powell, A. K. *Eur. J. Inorg. Chem.* **2005**, 692. (e) King, P.; Clérac, R.; Anson, C. E.; Coulon, C.; Powell, A. K. *Inorg. Chem.* **2003**, *42*, 3492. (f) Kostakis, G. E.; Mondal, K. C.; Abbas, G.; Lan, Y.; Novitchi, G.; Buth, G.; Anson, C. E.; Powell, A. K. *CrystEngComm.* **2009**, DOI: 10.1039/b905707b. (g) Abuhmaiera, R.; Lan, Y.; Ako, A. M.; Kostakis, G. E.; Mavrandonakis, A.; Klopper, W.; Clérac, R.; Anson, C. E.; Powell A. K. *CrystEngComm*, **2009**, *11*, 1089.

(18) (a) Liu, Y.-J.; Xiong, R.-G.; You, X.-Z.; Che, C.-M. *Z. Anorg. Allg. Chem.* **2004**, *630*, 2761. (b) Li, W.-G.; Pan, Z.-R.; Wang, Z.-W.; Li, Y.-Z.; Zheng, H.-G. *Acta Crystallogr., Sect. E* **2007**, *63*, m351. (c) Moncol, J.; Sega, P.; Jašková, J.; Fischer, A.; Melník, M. *Acta Crystallogr., Sect. E* **2007**, *63*, m698. (d) Zhou, Q.-X.; Wang, Y.-J.; Zhao, X.-Q.; Yue, L. *Chinese J. Struct.Chem.* **2004**, *23*, 570. (e) Gunning, N. S.; Cahill, C. L. *Dalton Trans.* **2005**, 2788. (f) Qiu., Z.-H.; Liang, F.-P.; Ruan, Q.-F.; Chen, Z.-L. *Acta Crystallogr., Sect. E* **2008**, *64*, m766. (g) Liu, C.-B.; Wen, H.-L.; Deng, F.; Zuo, J.-H. *Acta Crystallogr., Sect. E* **2008**, *64*, m201. (h) Tong, M.-L.; Chen, X.-M.; Batten, S. R. *J. Am. Chem. Soc.* **2003**, *125*, 16170. (i) Kurmoo, M.; Estournès, C.; Oka, Y.; Kumagai, H.; Inoue, K.*Inorg. Chem.* **2005**, *44*, 217. (j) Huang, Y.-G.; Zhou, Y.-F.; Wu, B.-L.; Han, L.; Yuan, D.-Q.; Lou, B.-Y.; Hong, M.-C. *Chin. J. Struct. Chem.* **2005**, *24*, 1123. (k) Jašková, J.; Mikloš, D.; Korabik, M.; Jorík, V.; Sega, P.; Kaliáková, B.; Hudecová, D.; vorec, J.; Fischer, A.; Mrozinski, J.; Lis, T.; Melník, M. *Inorg. Chim. Acta* **2007**, *360*, 2711. (l) Li, X.; Cao, R.; Sun, Y.; Bi, W.; Li, X.; Wang, Y. *Eur. J. Inorg. Chem.* **2005**, 321. (m) Wu, Q.; Huang, X.-F.; Zhou, T.; Tang, Y.-Z.; Xiong, R.-G. *Appl. Organomet. Chem.* **2005**, *19*, 189. (n) Yang, E.; Chen, Q.-Y.; Chen, G.-Y. *Acta Crystallogr., Sect. E* **2006**, *62*, m1043. (o) Miklovič, J.; Moncol, J.; Mikloč, D.; Sega, P.; Koman, M. *Acta Crystallogr., Sect. E* **2008**, *64*, m426. (p) Teoh, S. G.; Tan, D. S.; Yeap, G.-Y.; Fun, H.-K. *Z .Kristallogr.-New Cryst. Struct.* **1999**, *214*, 161.

(19) (a) Qu, Z.-R.; Zhao, H.; Wang, Y.-P.; Wang, X.-S.; Ye, Q.; Li, Y.-H.; Xiong, R.-G.; Abrahams, B. F.; Liu, Z.-G.; Xue, Z.-L.; You, X.-Z. *Chem.—Eur. J.* **2004**, *10*, 53. (b) Ayyappan, P.; Evans, O. R.; Lin, W. *Inorg. Chem.* **2001**, *40*, 4627. (c) Zhou, Q.-X.; Wang, Y.-J.; Song, H.-B.; Zhao, X.-Q. *Chin. J. Synthetic Crystals* **2003**, *32*, 451. (d) Wang, Y.-J.; Zhou, Q.-X.; Yue, L.; Zhao, X.-Q. *J. Coord. Chem.* **2004**, *57*, 741. (e) Zhou, Q.-X.; Wang, Y.-J.; Zhao, X.-Q.; Yue, L. *Chin. J. Inorg. Chem.* **2003**, *19*, 1245.

(20) (a) Zhou, Q.-X.; Bai, X.-J.; Chen, L.-P. *Chinese J. Struct. Chem.* **2006**, *25*, 49. (b) Song, Y.-M.; Shi, R.; Wang, X.-S.; Zhao, H.; Xiong, R.-G. *Appl. Organomet. Chem.* **2005**, *19*, 173. (c) Mondal, K. C.; Sengupta, O.; Nethaji, M.; Mukherjee, P. S. *Dalton Trans.* **2008**, 767.

Table 1. Comparison of Products with Various Reaction Conditions

M/L/base ratio	base	*T* (°C) (reaction time)	solvent	product	metal environment	coordination modes	space group	topology	ref
1:2:2	NaOH	180 (24 h)	H_2O	**2** [M = Co(II), Ni(II), Fe(II)]	*trans*-$O_4N_2(2H_2O)$	IVa, IVb	$P2_1/c$	**tcb (3D)**	18h
1:2:2	NaOH	150 (24 h)	H_2O	**3** M = Ni(II)	*cis*-$O_4N_2(2H_2O)$	IIa, Va	$P\bar{1}$	**1D**	18h
2:1:1	NaOH	120 (3d)	H_2O	**2** M = Co(II)	*trans*-$O_4N_2(2H_2O)$	IVb, IVc	$P2_1/c$	**tcb (3D)**	18i
2:1:1	NaOH	170 (3d)	H_2O	**3** M = Co(II)	*cis*-$O_4N_2(2H_2O)$	IIa, Va	$P\bar{1}$	**1D**	18i
1:2:excess	Pyridine	130 (24 h)	MeOH	**1** M = Co(II)	*cis*-$O_4N_2(H_2O)$	IVc, VIIIb	$C2/c$	**dia** (Co_2 unit as node) **(3D)**	19b
1:1:2	Et_3N	160 (4d)	H_2O	**4** M = Co(II)	*cis*-$O_4N_2(H_2O)$ *trans*-O_5N (H_2O)	IVc, VII, VIIIb	$P2_1/c$	**noz** (Co_2 unit as node) **pcu** (Co_4 unit as node) **(3D)**	this work
1:1:2:(0.2)	Et_3N (N-$^nBu_4NBr$)	160 (4d)	H_2O	**2** and **4** M = Co(II)	*cis*-$O_4N_2(H_2O)$ *trans*-O_5N (H_2O) and *trans*-$O_4N_2(2H_2O)$	IVc, VII, VIII and IVb, IVc	$P2_1/c$	**tcb** and **noz**	this work
1:1:2:(0.2)	Et_3N (N-$^nBu_4NBr$)	120 (24 h)	H_2O	**2** M = Co(II)	*trans*-$O_4N_2(2H_2O)$	IVb, IVc	$P2_1/c$	**tcb (3D)**	this work

center of symmetry and is coordinated to two *trans*-3-pyca via the pyridyl donors (Co−N = 2.214(2), 2.185(2) Å), two *trans*-3-pyca via the carboxylate donors (Co−O = 2.067(2), 2.125(2) Å), and two *trans* terminal water ligands (Co−O = 2.112(2), 2.086(2) Å). The structure of **3** consists of 1D chains of metal centers bridged by pyca ligands which coordinate through both the pyridyl (Co−N = 2.116(2) and 2.183(2) Å) and the carboxylate (Co−O = 2.160(2), 2.152(2) Å) functional groups, the latter in a chelating fashion. The remainder of the octahedral metal coordination sphere is composed of two *cis*-disposed water ligands (Co−O = 2.156(2), 2.008(2) Å). Both compounds are paramagnetic with Weiss constants suggesting weak interactions.[18h] The Curie constants are 3.353(4) cm^3 K/mol for **2** and 2.758(10) cm^3 K/mol for **3**. which are close to those expected for the ions in octahedral coordination environments with very weak exchange interactions, as also indicated by the Weiss constants, −24.1(3) K for **2** and +3(2) K for **3**. The positive value for **3** suggests ferromagnetic interactions between nearest neighbors. The isothermal magnetizations at 2 K behave as expected with saturation values of 2.21 μ_B for **2** and 2.75 μ_B for **3**, which lie in the range reported in the literature for paramagnetic cobalt complexes and is in agreement with an $S_{eff} = 1/2$ for cobalt.

It is well-known that the metal salt, temperature, solvent, and the time of reaction can all affect the nature of the final product. Bearing this in mind, we modified these parameters and observed the influence on the structural diversity of the final products. We present here a systematic study of the reaction of $CoCl_2$ with *trans*-3-pyacH and Et_3N using hydrothermal conditions which resulted in the formation of a new 3D compound formulated as $[\{Co_4(\mu\text{-}H_2O)_2(3\text{-pyca})_8\}_{0.94}\{Co_5(\mu_3\text{-}OH)_2(3\text{-pyca})_8\}_{0.06}]$ (**4**).

Experimental Section

General Information. All chemicals and solvents used for synthesis were obtained from commercial sources and were used as received without further purification. FTIR spectra were measured on a Perkin-Elmer Spectrum One spectrometer with samples prepared as KBr pellets. The X-ray powder diffraction patterns were measured at room temperature using a Stoe STADI-P diffractometer with Cu Kα radiation. For both compounds, phase purity was confirmed by comparison of the powder diffraction pattern of the bulk product with that simulated from the single crystal structure.

Syntheses of $[Co(3\text{-pyca})_2(H_2O)_2]$ (2) and $[\{Co_4(\mu\text{-}H_2O)_2(3\text{-pyca})_8\}_{0.94}\{Co_5(\mu_3\text{-}OH)_2(3\text{-pyca})_8\}_{0.06}]$ (4). $[Co(3\text{-pyca})_2(H_2O)_2]$ (2). An aqueous solution (10 mL) of $CoCl_2 \cdot 6H_2O$, *trans*-(3-pyridyl)-acrylic acid, Et_3N, and $^nBu_4NBr$ in the ratio of 1:1:2:0.2 was heated in a 20 mL Teflon autoclave and kept at 120 °C for 24 h. Cooling overnight led to the formation of small cubic pink crystals of **2** in 80% yield. Heating the same mixture to 160 °C in an autoclave for 4 days (i.e., the reaction conditions from the synthesis of **4** see below) followed by cooling overnight gave a mixture of the two products from which small dark pink crystals of **4** and large pink prisms of **2** can be isolated. These are easy to distinguish from each other and manually separate. Phase purity was checked with PXRD (see Supporting Information, Figure S3 and Table 1).

$[\{Co_4(\mu\text{-}H_2O)_2(3\text{-pyca})_8\}_{0.94}\{Co_5(\mu_3\text{-}OH)_2(3\text{-pyca})_8\}_{0.06}]$ (4). An aqueous solution (10 mL) of $CoCl_2 \cdot 6H_2O$, *trans*-(3-pyridyl)-acrylic acid (3-pycaH), and Et_3N in the ratio of 1:1:2 was heated in a 20 mL Teflon autoclave and kept at 160 °C for 4 days. Cooling overnight led to the formation of dark pink crystals of complex **4** in about 45% yield. Elemental analysis (%) Found: C 52.65; H 3.61; N 7.65; Calcd for $C_{64}H_{51.88}Co_{4.06}N_8O_{18}$: C 52.64; H 3.58; N 7.67. Selected IR data (KBr, ν/cm^{-1}): 3530 w, 3050 m, 2921 m, 1713, 1643 m, 1573 s, 1388, 1060 s, 881 ms, 806 and 711 m.

Table 2. Crystallographic Data and Structure Refinement for Compound **4**

formula	$C_{64}H_{51.88}Co_{4.06}N_8O_{18}$	D_c/Mg m^{-3}	1.603
formula weight	1460.28	M(Mo Kα)/mm^{-1}	1.176
crystal system	monoclinic	data measured	19631
space group	$P2_1/c$	unique data	8590
a/Å	10.2986(5)	R_{int}	0.0235
b/Å	24.0640(12)	data with $I \geq 2\sigma(I)$	7606
c/Å	12.8835(6)	wR_2 (all data)	0.0704
β/deg	108.614(1)	S (all data)	1.028
U/Å^3	3025.8(3)	R_1 [$I \geq 2\sigma(I)$]	0.0287
Z	2	parameters/restraints	432/2
T/K	100	biggest diff. peak/hole/eÅ^{-3}	+0.345/−0.496
F(000)	1491	CCDC number	728860

Magnetic Measurements. Magnetic susceptibility measurements were obtained using a Quantum Design SQUID MPMS-XL susceptometer. This magnetometer works between 1.8 and 300 K for direct current (dc) applied fields ranging from −7 to +7 T. Measurements for **4** were performed on 6.6 mg of a polycrystalline powder dispersed in 7.0 mg of Apeizon grease. The magnetic data were corrected for the sample holder and the diamagnetic contribution. The samples were first checked for the presence of ferromagnetic impurities by measuring the magnetization as a function of the field at 100 K, and none were detected.

X-ray Data Collection and Structure Determination. Data were collected at 100 K on a Bruker SMART Apex diffractometer using graphite-monochromated Mo Kα radiation. Crystals of **4** generally twin by a 180° rotation about the (real space) a-axis; data were integrated allowing for two twin domains and corrected for absorption using TWINABS.[21a] The structure were solved by direct methods followed by full-matrix least-squares refinement against F^2 (all data, HKLF 5 format) using SHELXTL.[21b] Non-H atoms were assigned anisotropic temperature factors; organic H atoms were placed in calculated positions, while coordinates of H atoms bonded to oxygen were refined.

Final refinement resulted in a mostly featureless (peaks <0.4 e Å^{-3}) difference map, except for a single large peak (ca. 3 e Å^{-3}) on the inversion center relating the two dinuclear $\{Co_2(\mu\text{-}OH_2)\}$ units. Given the low residuals for the structure and the otherwise rather flat difference map, this was considered unlikely to result from "errors accumulating on a special position" (the Gibbs effect). If one of the two aqua H-atoms, H(12), is removed, the centrosymmetric environment of the difference peak (six approximately octahedrally disposed oxygen atoms at 2.03−2.35 Å) is appropriate for a Co^{II} cation. Simultaneous refinement of the occupancy and isotropic temperature factor of a Co atom at this position always converged with an occupancy of about 6% and an isotropic temperature factor comparable to U_{eq} for Co(1) and Co(2). Similar results were found using crystals from other batches, and were also independent of the degree of twinning. Thus in 94% of the sites, there are the two $\{Co_2(\mu\text{-}OH_2)\}$ dinuclear units, while in the remaining 6% we have a pentanuclear $\{Co_5(\mu_3\text{-}OH)_2\}$ unit; the overall charge balance is unaffected.

The data collection and refinement are summarized in Table 2. Crystallographic data (excluding structure factors) for the structure in this paper have been deposited with the Cambridge Crystallographic Data Centre as supplementary publication nos. CCDC 728860. Copies of the data can be obtained, free of charge, on application to CCDC, 12 Union Road, Cambridge CB21EZ, U.K., http://www.ccdc.cam.ac.uk/cgi-bin/catreq.cgi, e-mail: data_request@ccdc.cam.ac.uk, or fax: +44 1223 336033.

Results and Discussion

Synthesis. All the compounds were synthesized using hydrothermal conditions from the reaction of $CoCl_2$, *trans*-3-pycaH and Et_3N as base in molecular ratio of 1:1:2 at 160 °C. A range of crystalline compounds with several different structural types have been already reported from this system,[18h,i,19b] depending on the reaction conditions. Compound **4** is a new product from this reaction matrix (see Table 1) and is stable and retains crystallinity even when exposed to air. Further experiments with different metal/ligand ratios were performed (3:1, 2:1, 1:1, 1:2, 1:3), and with different bases Et_3N or NaOH, as well as experiments extending the time duration and using different solvents (MeOH, EtOH). No new products were isolated. Additionally, reactions with other metal centers were performed. See the Supporting Information for details.

Structure Analysis. Compound **4** crystallizes in the monoclinic space group $P2_1/c$ and forms a neutral 3D framework. The asymmetric unit (for 94% of the structure, vide infra) comprises two Co^{II} centers bridged by an aqua ligand and four deprotonated *trans*-3-pyca anions as shown in Figure 1a. Both metal centers are coordinated in a rather regular octahedral geometry, although they possess different coordination environments. Three carboxylate-oxygens O(8), O(2), and O(4) and one pyridine-nitrogen N(3)^b atoms build the equatorial plane around Co(1) [the Co−O and Co−N equatorial bonds are 2.0434(10), 2.0957(11), 2.0431(10), and 2.1762(14) Å, respectively]. The apical positions are occupied by the bridging water molecule [Co(1)−O(1) 2.1796(11) Å] and one nitrogen atom from a different 3-pyca ligand [Co(1)−N(2) ^{a} 2.1509(13) Å], resulting in an O_4N_2 environment. Four carboxylate-oxygen atoms O(5), O(6), O(3), and O(9)^c occupy the equatorial positions with the Co−O bonds being 2.0592(11), 2.0879(11), 2.0948(11), and 2.1186(10) Å, respectively. Similar to Co(1), the apical positions of Co(2) are occupied by the bridging water molecule [Co(2)−O(1) 2.1839(11) Å] and a nitrogen from a different 3-pyca ligand [Co(2)−N(1) ^{d} 2.1277(13) Å], resulting in an O_5N environment. The axial Co−O bonds are longer than the equatorial Co−O ones. Selected bond distances and angles are depicted in Table 3. The degree of compression (s/h) and twisting angle (φ) for Co(1) and Co(2) are 56.80° and 1.259, 60.63° and 1.289 respectively (to be compared with those for the regular octahedron which are 60° and 1.22, respectively). The intramolecular distances $Co^{II}\cdots Co^{II}$ found in **4** are Co(1)−Co(2) 3.598, Co(1)−Co(2)^c 5.354, and Co(2)−Co (2)^c 5.233 Å.

(21) Sheldrick, G. M., *TWINABS 1.05*; Bruker AXS, Inc.: Madison, WI, 2006; (b) Sheldrick, G. M., *SHELXTL 6.12*; Bruker AXS, Inc.: Madison, WI, 2003.

(22) (a) Kostakis, G. E.; Casella, L.; Hadjiliadis, N.; Monzani, E.; Kourkoumelis, N.; Plakatouras, J. C. *Chem. Commun.* **2005**, 3859. (b) Habib, H. A.; Sanchiz, J.; Janiak, C. *Dalton Trans.* **2008**, 4877. (c) Shova, S. G.; Turyatke, L. G.; Novitchi, G; Mazus, M. D.; Gulya, A. P. *Russ. J. Coor., Chem.* **1996**, *22*, 485.

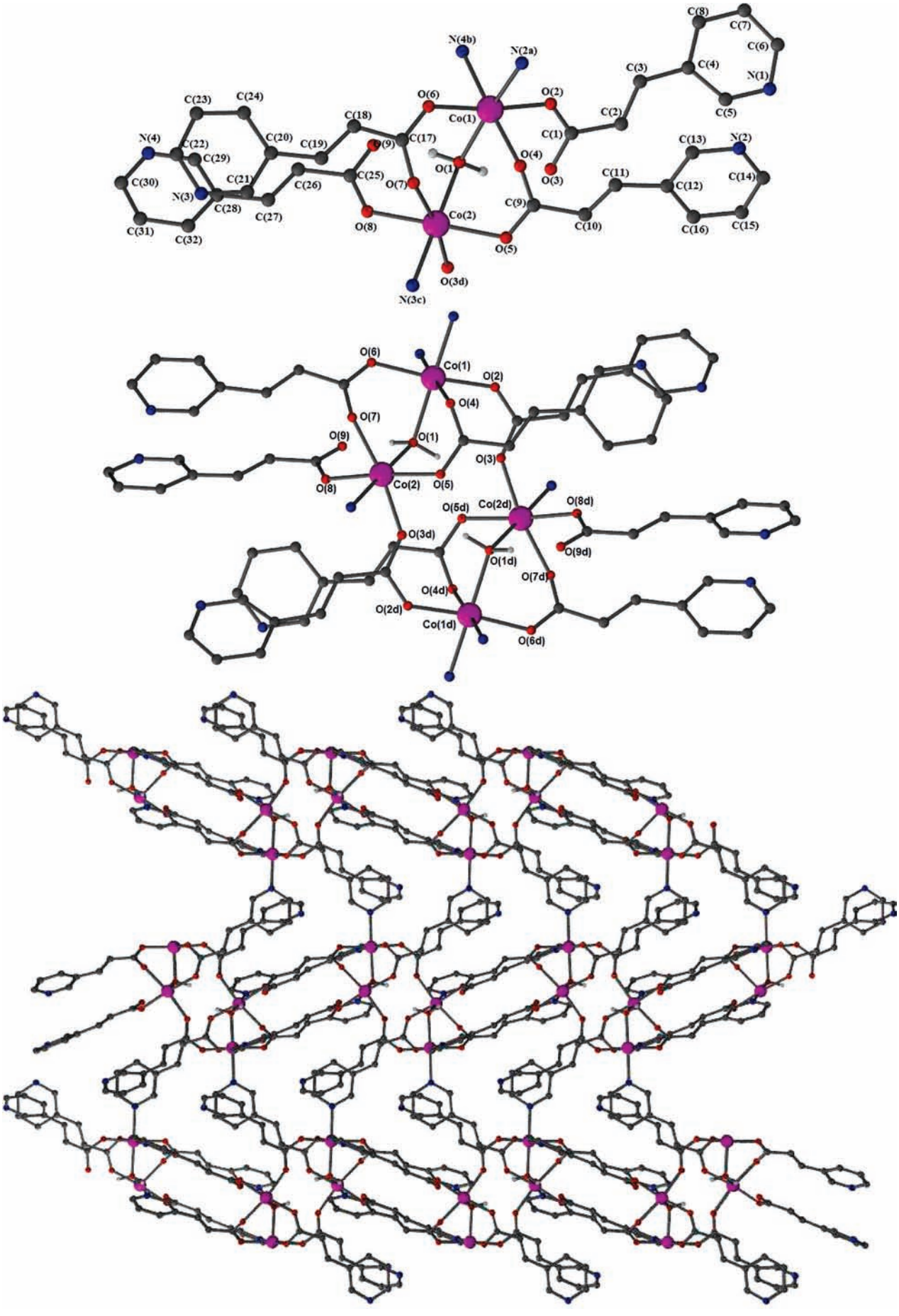

Figure 1. Asymmetric unit (upper), the embedded Co_4 unit (middle) and the 3D network (lower) in **4**. (Symmetry operations: *a*: x, $3/2-y$, $z-1/2$; *b*: $-x$, $1-y$, $1-z$; *c*: $-x-1$, $1-y$, $1-z$; *d*: $-x$, $1-y$, $2-z$).

Table 3. Selected Bond Distances and Angles in **4**

Co(1)−O(8)	2.0431(10)	N(2)^a−Co(1)−N(3)^b	94.09(5)
Co(1)−O(2)	2.0434(10)	O(8)−Co(1)−O(1)	94.32(4)
Co(1)−O(4)	2.0957(11)	O(2)−Co(1)−O(1)	90.09(4)
Co(1)−N(2)^a	2.1509(13)	O(4)−Co(1)−O(1)	86.61(4)
Co(1)−N(3)^b	2.1762(14)	N(2)^a−Co(1)−O(1)	173.86(5)
Co(1)−O(1)	2.1796(11)	N(3)^b−Co(1)−O(1)	91.92(5)
Co(2)−O(5)	2.0592(11)	O(5)−Co(2)−O(6)	172.77(4)
Co(2)−O(6)	2.0879(11)	O(5)−Co(2)−O(3)	104.70(4)
Co(2)−O(3)	2.0948(11)	O(6)−Co(2)−O(3)	81.99(4)
Co(2)−O(9)^c	2.1186(10)	O(5)−Co(2)−O(9)^c	83.97(4)
Co(2)−N(1)^d	2.1277(13)	O(6)−Co(2)−O(9)^c	89.49(4)
Co(2)−O(1)	2.1839(11)	O(3)−Co(2)−O(9)^c	170.95(4)
O(8)−Co(1)−O(2)	173.06(4)	O(5)−Co(2)−N(1)^d	93.29(5)
O(8)−Co(1)−O(4)	88.77(4)	O(6)−Co(2)−N(1)^d	89.54(5)
O(2)−Co(1)−O(4)	96.85(4)	O(3)−Co(2)−N(1)^d	89.02(4)
O(8)−Co(1)−N(2)^a	87.27(4)	O(9)^c−Co(2)−N(1)^d	87.86(4)
O(2)−Co(1)−N(2)^a	88.92(4)	O(5)−Co(2)−O(1)	87.27(4)
O(4)−Co(1)−N(2)^a	87.49(5)	O(6)−Co(2)−O(1)	89.66(4)
O(8)−Co(1)−N(3)^b	87.19(5)	O(3)−Co(2)−O(1)	92.86(4)
O(2)−Co(1)−N(3)^b	87.30(5)	O(9)^c−Co(2)−O(1)	90.11(4)
O(4)−Co(1)−N(3)^b	175.59(4)	N(1)^d−Co(2)−O(1)	177.83(5)
Co(1)···Co(2)	3.598	Co(2)···Co (2)^c	5.233
Co(1)···Co(2)^c	5.354		

^{a} Symmetry code: $x, -y+1/2, z-1/2$. ^{b} Symmetry code: $-x+1, -y+1, -z$. ^{c} Symmetry code: $-x+1, -y+1, -z+1$. ^{d} Symmetry code: $-x, -y+1, -z$.

The Co−O geometries within the aqua bridge, with Co(1)−O(1) 2.1796(11) and Co(2)−O(1) 2.1839(11) Å and the angle Co(1)−O(1)−Co(2) 111.09(5)°, are in good agreement with similar water bridges,[22] and the two hydrogen atoms could be easily located and refined. The four ligands adopt three different coordination modes IVc, VII, and VIIIb (see Scheme 1). Two of them are bonded to two metals and the other two to three metal centers. Overall, the elongated pyridyl ligands with coordination by their nitrogen atoms are responsible for the composition of the neutral 3D network. Thus, two $\{Co^{II}_2(H_2O)\}$ units are connected by *syn-anti* carboxylate into an Co^{II}_4 unit, and all Co^{II} ions of the Co^{II}_4 unit are in the same plane.

As mentioned in the experimental details, during the final stages of refining the structure of **4**, one single large difference peak (ca. 3 e Å^{-3}) was found on the inversion center relating the two dinuclear $\{Co_2(\mu\text{-}H_2O)\}$ units. Closer inspection of the environment of the peak, with six approximately octahedrally disposed oxygen atoms at 2.03−2.35 Å, showed that it is appropriate for a Co^{II} cation. Simultaneous refinement of the occupancy and isotropic temperature factor of a Co atom at this position always converged with an occupancy of about 6% and an isotropic temperature factor comparable to U_{eq} for Co(1) and Co(2). Similar results were found using crystals from other batches and were also independent of the degree of twinning. If two hydrogen atoms, H(12) and H(12′), one from each of the two aqua bridges are replaced by this extra partial Co then the two $\{Co_2(\mu\text{-}H_2O)\}$ dinuclear units become a pentanuclear $\{Co_5(\mu_3\text{-}OH)_2\}$ unit with plausible geometry, while the overall charge balance remains unaffected (Figure 2). Thus 94% of the sites contain the two $\{Co_2(\mu\text{-}H_2O)\}$ dinuclear units as described above, while in the remaining 6% we have the pentanuclear unit. We are unaware of any other examples of such disorder in the literature.

Phase purity of the bulk material was confirmed by comparison of its powder diffraction pattern with that calculated from the single-crystal study (Figure 3). There is no detectable difference between the simulations from the single crystal data for **4** assuming 100% Co_4 or using the 94% to 6% distribution of Co_4 and Co_5.

A compound with a similar structural unit has been previously reported by Lin;[19b] however, substantial differences in the coordination environment of the metal centers and the ligand results in a different architecture for the overall compound. Compared to Lin's compound, **4** has two independent metal centers with different environments instead of one, the ligands adopt three different coordination modes instead of two with the ligand in the VII coordination mode bridging two dinuclear units and embedding the tetranuclear unit, the bridging water ligand forms two hydrogen bonds (to the carboxylate oxygen atoms O7 and O9) reinforcing the tetranuclear unit and playing an important role in directing the network topology, and has no "free volume" for guest molecules.

Topological Analysis. There are two possible scenarios for the topological analysis of the 3D network of **4**. The first involves the dimeric units (Co_2) and the second the embedded tetramer (Co_4). Taking into account the Co^{II}_2 dimer as a node, the network can thus be presented topologically simply by the Co_2 nodes and the connections (bridging 3-pyca ligands) between them. Figure 4 depicts the network resulting from this analysis. The net is a rare 5-connected ($4^4.6^6$) **noz** structure with a literature survey[23] revealing only seven other examples and is the first derived from the *trans*-3-pyca ligand. If we take the tetrameric unit as a node and the bridging ligands as connections, then the topology can be described in terms of a **pcu** (NaCl) 6-connected network.

When $CoCl_2$/*trans*-3-pycaH/Et_3N in a molar ratio of 1:1:2 are reacted at 160 °C in the presence of $^nBu_4NBr$ (0.2 equiv), two different kind of crystals are obtained, which were identified by powder diffraction. The small pink crystals were found to be compound **4**, with larger red crystals identified as the previously reported [Co(3-pyca)$_2$(H$_2$O)$_2$] (**2**).[18h,i] This observation indicates that addition of $^nBu_4NBr$ encourages the ligation of all the nitrogen atoms with reorganization of the coordination network into the alternative morphology. From a systematic study of this cobalt/ligand/base system, all analogous reactions at lower temperature (120 °C) gave only compound **2**, in agreement with previous reported results.[18h] However, we note that reactions in the presence of $^nBu_4NBr$ generally produce crystals of **2** that are much larger than those obtained in the absence of $^nBu_4NBr$. All results from this work compared with previously reported results are listed in Table 1.

Magnetic Properties. The magnetic studies were carried out on a powder sample dispersed in Apeizon grease. The temperature dependence of the molar magnetic susceptibility of complex **4** at various fields is shown in Figure 5.

(23) O'Keeffe, M.; Peskov, M. A.; Ramsden, S. J.; Yaghi, O. M. *Acc. Chem. Res.* **2008**, *41*, 1782. For further compounds with noz topology see also: NIGHOA, Wu, L. P.; Yamagiwa, Y.; Kuroda-Sowa, T.; Kamikawa, T.; Munakata, M. *Inorg. Chim. Acta*, **1997**, *256*, 155; QIBTAW, Long, D.-L.; Blake, A. J.; Champness, N. R.; Wilson, C.; Schröder, M.; *J. Am. Chem. Soc*., **2001**, *123*, 3401 MIGVON, MIGVUT, Ponomarova, V. V.; Komarchuk, V. V.; Boldog, I.; Chernega, A. N.; Sieler, J.; Domasevitsch, K. V. *Chem. Commun*., **2002**, 436. CIKGUZ, CIKHAG, XUWWAN.

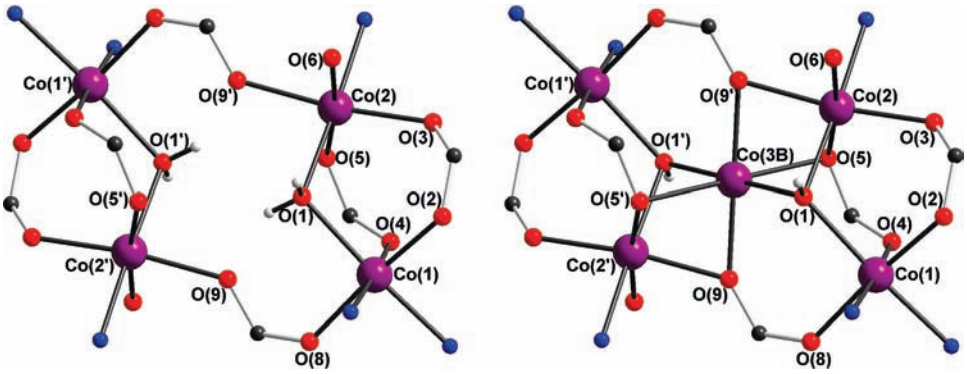

Figure 2. Linkage of two $\{Co_2(\mu\text{-}H_2O)\}$ dinuclear units via carboxylate bridges in the major (94%) component of the structure (left); replacement of two hydrogens on the aqua ligands with a Co^{II} on the inversion center gives a pentanuclear $\{Co_5(\mu_3\text{-}OH)_2\}$ unit in the minor (6%) component.

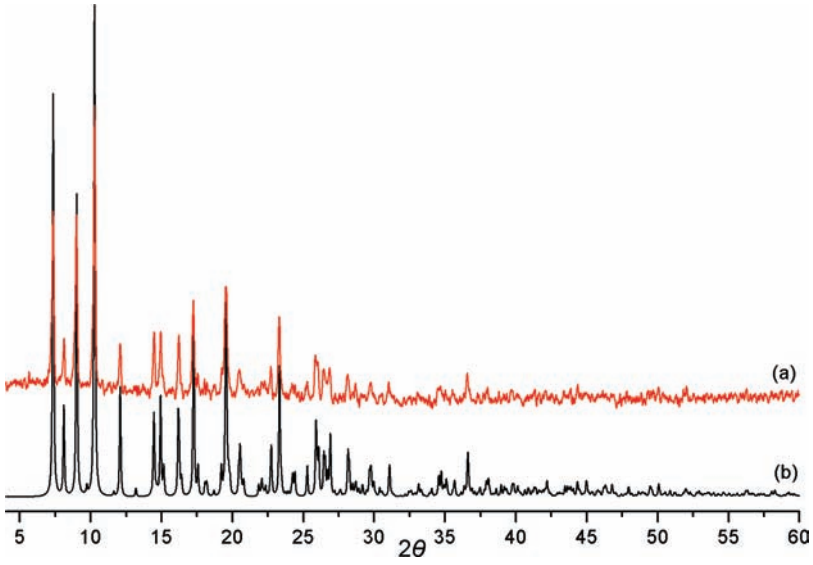

Figure 3. X-ray powder diffraction patterns for compound **4**: (a) simulated for the major component (see text); (b) experimental.

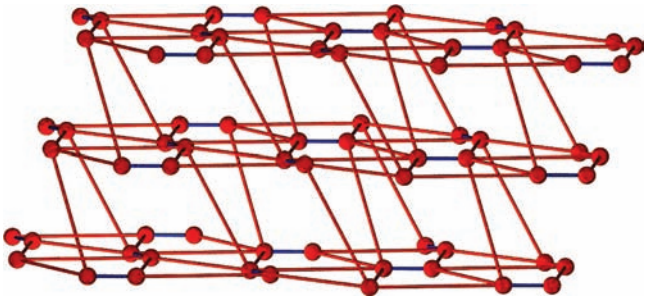

Figure 4. Topological representation of the 5-connected net with topology **noz**. Bonds in blue represent the short linkages between dinuclear Co_2 units.

The room temperature χT value for this compound under an applied field of 1000 G is 12.11 cm^3 K mol^{-1} which is much higher than that of the spin only value of 7.61 cm^3 K mol^{-1} for 94% $Co^{II}{}_4$ and 6% $Co^{II}{}_5$ (Co^{II}; $S = 3/2$ and $g = 2.0$) indicating the presence of an orbital contribution.[24] The χT value gradually decreases with decreasing temperature and reaches a minimum of 6.70 cm^3 K mol^{-1} at 13 K. On cooling further the χT value rapidly increases to come to a maximum at 9.5 K and then sharply falls to 1.80 cm^3 K mol^{-1}at 1.8 K. This type of magnetic behavior

(24) Robinson, W. K.; Friedberg, S. A. *Phys. Rev.* **1960**, *117*, 402.

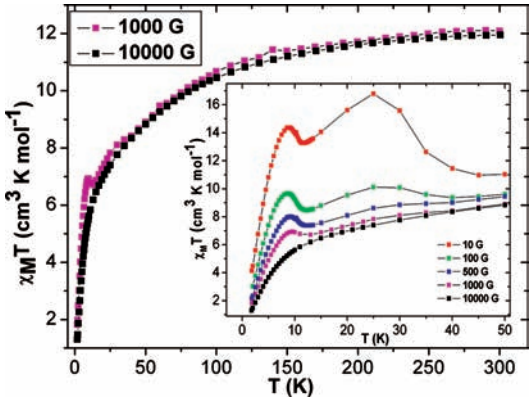

Figure 5. $\chi_M T$ vs T plots at the indicated applied magnetic fields; inset, below 50 K.

is characteristic of a ferrimagnetism or canted antiferromagnetism as reported extensively before.[11−13] The final decrease of the χT value suggests the presence of intermolecular interactions and/or magnetic anisotropy of Co^{II} ions.[8,13] A fit of the experimental data to the Curie−Weiss law above 40 K gives a Curie constant, C, of 13.26 cm^3 K mol^{-1} and a Weiss temperature, θ, of −24.08 K. The negative θ value may indicate the presence of overall antiferromagnetic interactions within

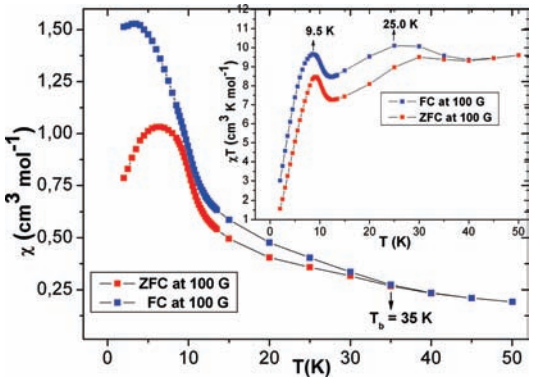

Figure 6. ZFC and FC plots at 100 G; inset: $\chi_M T$ vs T plot.

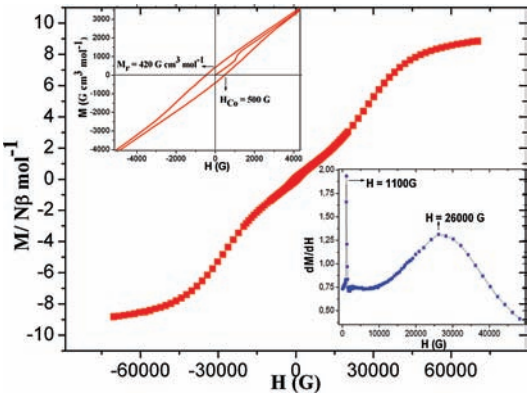

Figure 7. Hysteresis loop at 1.8 K; inset, left: zoom of the loop; inset, right: dM/dH vs H plot.

the Co^{II} centers in addition to the spin−orbit coupling effects of Co^{II} ions. It is noticeable that another peak centered at 25 K starts appearing when the applied static field is less than 1000 G, and it becomes more pronounced when the field decreases down to 10 G (Figure 5, inset). In addition, both the maxima in χT values at different applied fields as a function of temperature show the same field-induced response below 40 K, which is more noticeable for lower field strengths. These results are in line with those previously reported canted antiferromagnetic systems.[8,11−13] The field-cooled (FC) and zero-field-cooled (ZFC) magnetizations were measured at 100 G upon warming from 2 K (Figure 6). The ZFC and FC susceptibilities diverge around 35 K and intend to be superposed from 11 to 9 K and then completely open up below 9 K. The critical temperatures (T_c) ascertained in the ZFC and FC plots are consistent with those observed in the temperature dependence of susceptibilities both alternating current (ac) at zero field and dc at various fields (see Supporting Information). This observation suggests that one magnetic phase transition clearly appears in this compound, but it might be somehow disturbed leading to two possible magnetic domains. Considering the structure of **4**, the small percentage of the Co_5 unit occupying in each unit cell might be responsible for this perturbation. This will be discussed further in the following text.

The magnetization at 1.8 K first increases slowly with H, as for a typical antiferromagnet, and then increases abruptly above 1000 G (Figure 7). Above 40000 G it increases slowly again, reaching a value of 8.12 Nβ at 70000 G without showing true saturation.[25−27] The plots of M versus H/T at different temperatures (see Supporting Information) do not superpose on to a single master curve, indicating the presence of significant anisotropy and/or the population of low-lying excited states.[28,29] The sigmoidal shape of M versus H plot at 1.8 K suggests the presence of metamagnetic behavior.[7,13] The critical field values are about 1100 and 26000 G and correspond to the field at which a maximum in the dM/dH value is reached (Figure 7, inset right). The complex **4** exhibits a hysteresis loop at 1.8 K with a coercive field of 500 G (Figure 7, inset left). Extrapolation of the high field linear part of the magnetization curve to zero field gives a remanent magnetization of 420 G cm^3 mol^{-1} (0.075 Nβ). The canting angle can then be calculated as[10] $\alpha = \tan^{-1}(M_r/M_s) = 0.54°$, where $M_s = 8.12$ Nβ.

The ac susceptibility measurements at zero applied dc field and at 997.34 Hz frequency show the presence of an in-phase susceptibility (χ') signal while the out-of-phase signal (χ'') is negligible (see Supporting Information), which is probably the result of the small canting angle.[30] That is, the magnetization is almost canceled when the spin carriers are antiferromagnetically coupled and only slightly canted. In short, all these features indicate that compound **4** is a molecular metamagnet built of spin-canted antiferromagnetic units.

The neighboring Co^{II}_4/Co^{II}_5 units in the network are separated by 8.7 Å through the hydrocarbon skeleton of the carboxylate ligand, and thus the effective magnetic pathways are likely to be dominant by the tetranuclear core. The tetranuclear core of **4** is built up from dimeric $\{Co^{II}_2(H_2O)\}$ units through double *syn-anti* bridged carboxylates (Figure 1 and 2). Weak antiferromagnetic interactions are expected to be mediated through this mode as frequently reported previously and these are usually in the range of −3 to −1 cm^{-1}.[31] When the interactions are weak enough, they can be overcome upon increasing the external applied field. In line with the M versus H plot (Figure 7), two critical fields (1100 and 26000 G) are unambiguously observed in this material. Thus, the origin of metamagnetic behavior in compound **4** can be attributed to the weak AF interactions present in each dimeric $\{Co^{II}_2(H_2O)\}$ unit as well as within the tetranuclear core. However, the magnitude of the AF interactions in the latter case should be even smaller than the former one. Therefore, the smaller critical field at 1100 G can be assigned as that which overcomes the interactions

(25) Mabbs, F. E.; Machin, D. J. *Magnetism and Transition Metal Complexes*; Chapman and Hall: London, 1973.
(26) Peddis, D.; Mansilla, M. V.; Mørup, S.; Cannas, C.; Musinu, A.; Piccaluga, G.; D'Orazio, F.; Lucari, F.; Fiorani, D. *J. Phys. Chem. B* **2008**, *112*, 8507.
(27) Benelli, C.; Gatteschi, D. *Chem. Rev.* **2002**, *102*, 2369.
(28) Kahn, M. L.; Sutter, J.-P.; Golhen, S.; Guionneau, P.; Ouahab, L.; Kahn, O.; Chasseau, D. *J. Am. Chem. Soc.* **2000**, *122*, 3413.
(29) Yuan, M.; Zhao, F.; Zhang, W.; Wang, Z.-M.; Gao, S. *Inorg. Chem.* **2007**, *46*, 11235.
(30) See for example: (a) Yoon, J. W.; Jhung, S. H.; Hwang, Y. K.; Humphrey, S. M.; Wood, P. T.; Chang, J. S. *Adv. Mater.* **2007**, *19*, 1830. (b) Chen, B. L.; Ma, S. Q.; Zapata, F.; Fronczek, F. R.; Lobkovsky, E. B.; Zhou, H. C. *Inorg. Chem.* **2007**, *46*, 1233.
(31) (a) Delgado, F. S.; Hernández-Molina, M.; Sanchiz, J.; Ruiz-Pérez, C.; Rodríguez-Martín, Y.; López, T.; Lloret, F.; Julve, M. *CrystEngComm.* **2004**, *6*, 106. (b) Liu, H.; Song, L.-J.; Ju, Z.-F.; Li, W.; Zhang, J. *J. Mol. Struct.* **2008**, *875*, 565.

present within the tetranuclear core while the point at 26000 G is where the *syn-anti* bridged dimeric $\{Co^{II}_2(H_2O)\}$ unit interactions are overcome. Furthermore, within each $\{Co^{II}_2(H_2O)\}$ unit, the two Co^{II} ions are asymmetric, and connected by two *syn-syn* carboxylato and one μ-aqua bridges. To take spin-canting into account two factors need to be considered: the antisymmetric component of the superexchange interaction (Dzyaloshinsky−Moriya interaction, DMI) and the magnetic anisotropy.[32] Since Co^{II} is an Ising-type ion with significant anisotropy, the canting in **4** may occur in the asymmetric Co^{II} dinuclear unit along each dimension. When an additional Co^{II} is encapsulated in the tetranuclear core giving the pentanuclear 6% component, the Co^{II} ion can be tilted toward both dinuclear units squashing the canting angle slightly. However, since only a small percentage (6%) is occupied by the additional Co^{II} ion, the main magnetic phase associated with the moiety of $\{Co^{II}_2(H_2O)\}_2$ is only manifested as a perturbation in the magnetic data as shown in the ZFC-FC plot (Figure 6). Overall, compound **4** is a new 3D network exhibiting coexistence of spin-canting and metamagnetic behavior, which is not uncommonly observed in some networks containing Mn^{II} and Co^{II} ions.[33]

(32) Lloret, F.; Munno, G.; De Julve, M.; Cano, J.; Ruiz, R.; Caneschi, A. *Angew. Chem., Int. Ed.* **1998**, *37*, 135.

(33) (a) Gao, E.-Q.; Wang, Z.-M.; Yan, C.-H. *Chem. Commun.* **2003**, 1748. (b) Wang, X.-Y.; Wang, L.; Wang, Z.-M.; Su, G.; Gao, S. *Chem. Mater.* **2005**, *17*, 6369. (c) Ko, H. H.; Lim, J. H.; Kim, H. C.; Hong, C. S. *Inorg. Chem.* **2006**, *45*, 8847. (d) Zeng, M.-H.; Zhang, W.-X.; Sun, X.-Z.; Chen, X.-M. *Angew. Chem., Int. Ed.* **2005**, *117*, 3139.

Conclusion

The reaction of the $CoCl_2$ with and Et_3N at hydrothermal conditions results in the formation of a new 3D compound formulated as $[\{Co_4(\mu\text{-}H_2O)_2(3\text{-pyca})_8\}_{0.94}\{Co_5(\mu_3\text{-}OH)_2(3\text{-pyca})_8\}_{0.06}]$. Topologically, the 3D net can be considered as a rare 5-connected **noz** or a 6-connected **pcu** network. The magnetic measurements show that the complex exhibits the combination of the spin-canting and metamagnetic phenomena below the critical temperature of 9.5 K. In addition, the system shows a hysteresis loop characteristic of a magnet with a coercive field of 500 G and a remanent magnetization of 0.075 Nβ.

Acknowledgment. The authors are grateful to the EU network MAGMANet (NMP3-CT-2005-515767) and the DFG Center for Functional Nanostructures for financial support. We thank Prof. G. M. Sheldrick for a helpful discussion regarding the partial-occupancy Co atom.

Supporting Information Available: χ versus T at various applied fields and M versus H/T for compound **4**. This material is available free of charge via the Internet at http://pubs.acs.org.